Prod. Eng. Res. Devel. (2017) 11:731–743
DOI 10.1007/s11740-017-0767-y

ASSEMBLY

Biomimetic design of an ultra-compact and light-weight soft muscle glove

Zhejun Yao[1] · Christine Linnenberg[1] · Andreas Argubi-Wollesen[1] · Robert Weidner[1] · Jens P. Wulfsberg[1]

Received: 10 April 2017 / Accepted: 19 September 2017 / Published online: 26 September 2017

Abstract Wearable robotic hand devices can support people doing hand-intensive tasks by reducing the physical stress and strain on the human hand. For the safety and comfort of the user, such a device should be compatible and inconspicuous. Based on these two requirements, this paper presents a biomimetic design of a wearable robotic hand device called *soft muscle glove*, aiming to restore the salient features and functionalities of the human hand. Inspired by the hand musculature, the soft structure of the glove contains strings, bands and shape memory alloy (SMA) spring actuators to replicate the functionalities of tendons, pulleys and muscles in the human hand. The low-mass and small-size SMA spring actuator allows an ultra-compact and light-weight design of the glove with high dexterity. The glove weighs in total 85.03 g inclusive of the actuators and microcontroller. The performance of the muscle glove was experimentally investigated through hand function tests. The experimental results suggest that the glove can achieve functional range of motion of the human hand and can perform a wide range of grasp types defined in grasp taxonomy. Moreover, the grasping performance of the muscle glove with coupled and uncoupled flexion of the finger joints was compared. The uncoupled control shows a better matching between the grasp posture and the objects form, contributing to more efficient force transmission. This confirms the benefits of the proposed highly biomimetic design.

Keywords Soft wearable robotic glove · Biomimetic design · Shape memory alloy · Ultra-compact · Light-weight

1 Introduction

Even at a high level of automation, the modern industry still involves a large number of tasks that need to be performed by a human operator. According to the Fifth European Working Conditions Survey in 2010, workers remain exposed to physical hazards as they did 20 years ago [1]. Most of the hazardous manual tasks are strongly associated with the hand, e.g. over 60% workers in industrial production are working with repetitive hand and arm movements, while 33% workers carry heavy loads in more than 25% of their working time. These repetitive and strenuous hand-intensive tasks are key risk factors for work-related musculoskeletal disorders (WMSDs) of the hand and wrist [2]. WMSDs are the main causes (over 30%) of sickness absences from work and about 15% of the WMSDs are associated with hand and wrist [3]. Despite ergonomic improvement of working space and working tools, wearable robotic (WR) devices, like exoskeletons and active orthotics, appear to be a new solution for preventing WMSDs. These devices are worn by the users and support the users directly by reducing musculoskeletal stress and strain, e.g. on knee [4], shoulder [5] and hand [6, 7]. A well designed WR device should primarily meet the following two requirements: (1) the device should be compatible with users natural motion, i.e. not limit or alter the natural motion and restore it as truly as possible; (2) it should be as inconspicuous as possible in both weight and size, i.e. the device should not add excess load and volume to the user. These two requirements are extremely

✉ Zhejun Yao
zhejun.yao@hsu-hh.de

Robert Weidner
robert.weidner@hsu-hh.de

[1] Laboratory for Manufacturing Technology, Holstenhofweg 85, 22043 Hamburg, Germany

challenging for the WR hand devices because of the high level dexterity of the human hand and the lack of space around the hand, especially between the fingers. Although many efforts have been made in previous works to fulfill these two requirements as much as possible, there is still significant room for improvement.

In this paper, a soft WR glove is presented that aims to be compatible and inconspicuous at an unprecedented level. The proposed design, based on the concept of human hybrid robot [8], aims to be an ultra-compact and lightweight soft glove achieving human-level dexterity. As shown in Fig. 1, the glove contains a soft structure inspired by the hand musculature, using strings, bands and SMA spring actuators to mimic the functionalities of tendons, pulleys and muscles in the human hand. It has 14 active degrees of freedom (DOF) for four digits (the little finger is not involved). Thanks to the SMA spring actuator the whole glove, inclusive of actuators and microcontroller, weighs only 85 g. The fastening tapes on the sleeve allow simple adjustment for variations in wrist and arm sizes. The primary targeted applications of the muscle glove are repetitive handgrip tasks in assembly line, which are performed during prolonged period with low contraction force. The muscle glove aims to reduce muscle fatigue and provide enough recovery time for the workers by reducing muscle contraction force and time in defined work–rest cycles. Additionally, the muscle glove can be potentially used for supporting hand-intensive tasks in daily life, functional compensation for elderly people, in rehabilitation and in space suits.

In the following sections, related work is first reviewed to position our proposed design. And then the biomimetic design of the muscle glove based on the important anatomical features of the hand is detailed. After this, the design and control of the SMA spring actuator is discussed. Finally, the performance of the muscle glove is experimentally investigated through hand function tests to demonstrate the benefits received from the highly biomimetic design.

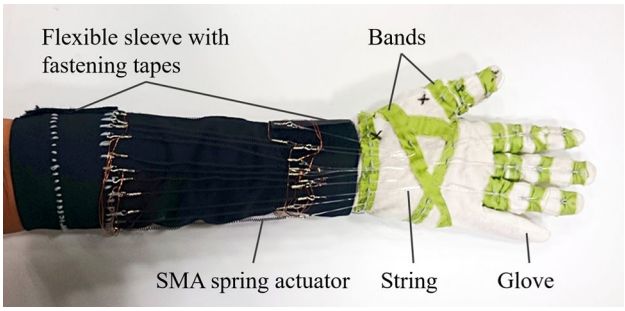

Fig. 1 Photograph of the muscle glove (first prototype) with flexible sleeve

2 Related work

In perspective of the two requirements described above, in this section the most relevant past work in WR devices for the hand is briefly reviewed, and the contribution of our design method is introduced.

In previous work, the majority of WR hand devices which support hand movements are developed for hand rehabilitation. ExoHand (Festo) [7] and RoboGlove (NASA and General Motor) [6] are two examples of industrial application, providing grasping support. State of art WR hand devices can be mainly classified into two groups depending on their design concepts (see Table 1). The first group mechanize the anatomical structure of the hand by using mechanical linkages to build up an external skeleton attached to the user, e.g. [7, 9–14]. The user's inherent skeleton is moved by the actuated exoskeleton. In contrast, the second group do not have a rigid skeletal structure, but take the user's skeleton as their supporting structure and mimic the biological actuation mechanism of the hand, e.g. soft gloves with tendon-driven mechanisms [6, 15–17] or soft elastomeric actuators [18, 19]. As mentioned above, one of the most important issues in exoskeleton design is the compatibility between the biological and the mechanical skeleton. Kinematic incompatibilities are mainly caused by misalignments between biological joint axes and mechanical joint axes, which can lead to discomfort and disturb the natural movement of the wearer [20]. Misalignments and their negative effects can be reduced by proper kinematic design of the exoskeleton structure. One of the solutions is to place the exoskeleton joint aside the anatomical finger joint and coincide their rotation axes, e.g. [9, 10]. However, the mechanical links between the fingers decrease the range of motion (ROM) of the fingers in abduction/adduction, and especially prevent the fingers moving close to their neighboring fingers. An alternative design is to locate the exoskeleton finger parallel to the biological finger at its back side. Each exoskeleton finger is a serial kinematic chain which is attached to every phalange of the supported finger [7, 11–13] or only to the fingertip [14]. They share the same kinematic feature of flexible joint rotation axis which is parallel to the biological joint axis and can move coincidently with the biological joint axis. In this way, the negative effect of misalignment is avoided.

The WR hand devices in the second group bypass the problem of misalignment by building no extra skeletal structure but involve the users skeletal structure in the device for desired motion. Soft elastomeric actuators are frequently used in these devices, e.g. [18, 19]. The soft actuators are mainly attached to the backside of a glove, and each finger is independently controlled by one actuator (except the thumb), but the joints motion of each finger is coupled. For a higher level of dexterity more actuators are needed. Compared with the exoskeletons with

Table 1 Classification of the reviewed WR hand devices according to their design concept

	References	Force transmission	Kinematic compatibility	Space requirement of the structure	Actuator	Location of actuator
Group 1: WR devices with mechanical skeleton						
Mechanical joints locate aside the finger joints	[9, 10]	Cable or linkage	Requiring coincidence between biological and mechanical joint rotation axis	Additional space around or between fingers	Motor	Not wearable
Mechanical joints locate above the finger joints	[7, 11–14]	Cable or linkage	The mechanical joint rotation axis should be flexible and can move coincidently with the biological joint axis	Additional space at the backside of fingers and hand	Motor or pneumatic actuator [7]	Above the hand [7, 14] or not wearable [11–13]
Group 2: WR devices without mechanical skeleton						
Soft elastomeric actuator placed over the finger	[18, 19]	Direct actuation	Inherently compatible	Additional space at the backside of fingers and hand	Soft elastomeric actuator	Above the fingers or in hand area
Soft glove with tendon-driven mechanism	[6, 15–17]	Cable	Inherently compatible	Depending on the gloves size and its routing system	Motor	Forearm [6], on torso [15, 17] or not wearable [16]

rigid structures, the soft robotic gloves with elastomeric actuators have advantages for safety, comfort and portability due to their soft and compact structure. However, the soft actuator still requires additional space around the hand which means collision-free workspace of the hand is reduced by wearing the glove-type WR device in a closed environment, especially in narrow working space which, for example, normally fit only one hand wearing a normal working glove. This can be resolved by soft gloves with tendon-driven mechanism [6, 15–17]. These WR gloves contain cables which functionally mimic the tendons in human hand and use electric motors located away from the hand to pull the cables. The hand is, thus, free from excess volume caused by mechanical linkages and actuators. This is a great advantage in comparison to the other types of WR hand devices.

The total weight and size of a WR device is strongly associated with its actuators. Most state of the art WR hand devices use underactuated mechanisms, in which the number of active DOF is lower than the inherent DOF of the system. Thus, only a small number of actuators are required and this leads to simplification of design and control. However, it inhibits the preservation of complete fine motor skills of the hand and prevents a wider application of the WR devices. In order to fulfill the requirement of rehabilitation exercise, flexing and extending each finger joint independently, Wege et al. developed the first hand exoskeleton with human-level dexterity [12]. However, the high dexterity costs large size and weight as a result of more motors. Balancing the dexterity and inconspicuousness is generally a challenge for WR hand devices with pneumatic actuators or electric motors. Shape memory alloy (SMA) provides an alternative way to cope with this problem. Dittmer et al. applied SMA wire to a wrist-hand orthotic with a rigid structure, leading to miniaturization and a light-weight design [21]. The SMA wire can provide high recovery force but very small stroke length. SMA spring actuator provides larger stroke and is more popular as a stand-alone actuator. However, the hysteresis and the fatigues of the SMA should be considered by actuator design and control. Tradeoffs are required in terms of energy consumption and response time of the SMA actuator. Those terms will be discussed in Sect. 4.

Based on the findings above, it was proposed to combine tendon-driven mechanism and SMA spring actuators for an ultra-compact and light-weight design. The state of the art tendon-driven mechanisms simplified the tendon anatomy of the human hand, as their WR gloves mainly focus on augmentation of grasping force. In contrast to them, our proposed design better replicates the tendon anatomy of the human hand, aiming to truly restore the natural hand movements. This study is the first attempt to thoroughly transfer the mechanism of human hand musculature to a soft WR glove. This highly biomimetic design method will have

potential impact on studies in clothing-type WR devices and active prostheses.

3 Design of the muscle glove

In this section, the design concept is described with the understanding of the hand anatomy in engineering point of view from three aspects: skeleton, tendons and muscles, and pulleys. The important biomechanical features and functionalities of the human hand musculature are identified, and the way to realize these functions is explained.

3.1 Hand skeleton

The design of the muscle glove, especially the soft force transmission structure (the bands and the strings), is based on the hand skeleton. A hand has five digits: one thumb and four fingers (index, middle, ring and little finger). Each finger has three phalangeal bones (distal, middle and proximal), one metacarpal bone, and three active joints which are the distal interphalangeal joint (DIP), the proximal interphalangeal joint (PIP) and the metacarpophalangeal joint (MCP) (see Fig. 2). The thumb has two phalanges and one metacarpal bone, with the interphalangeal joint (IP), the metacarpophalangeal joint (MCP) and the carpometacarpal joint (CMC). The muscle glove contains, for the finger, three active DOF for the flexion/extension of the three finger joints and one passive DOF for abduction/adduction at MCP joints. The thumb movements permitted by the glove are flexion/extension at the three thumb joints, abduction/adduction at MCP and CMC joint.

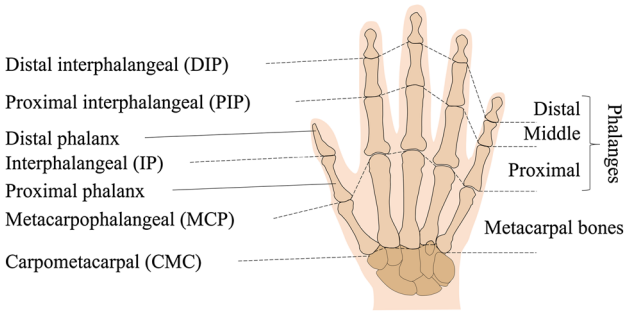

Fig. 2 Schematic of a hand skeleton (modified from [22])

3.2 Tendons and muscles

Tendons are soft tissues which connect muscle to bone and transmit muscle force. We use SMA spring actuators and nylon strings to imitate muscles and tendons. The nylon string has a diameter of 0.35 mm and a maximum load of 3.5 kg. The flexor tendon systems of a human left hand and its corresponding glove are illustrated in Fig. 3. Flexor digitorum profundus (FDP), flexor digitorum superficialis (FDS) and interosseous (IOs) are flexor muscles of the hand and are mainly responsible for finger flexion. FDP and FDS are two extrinsic flexors which locate on the forearm and insert into finger phalanges through their corresponding tendons, while IOs are intrinsic muscles of the fingers and locate directly in the palm of the hand. In order to minimize the thickness of the glove part, all the intrinsic muscles are treated as extrinsic muscles for the muscle glove, consisting of strings located in glove part and SMA spring actuators attached to

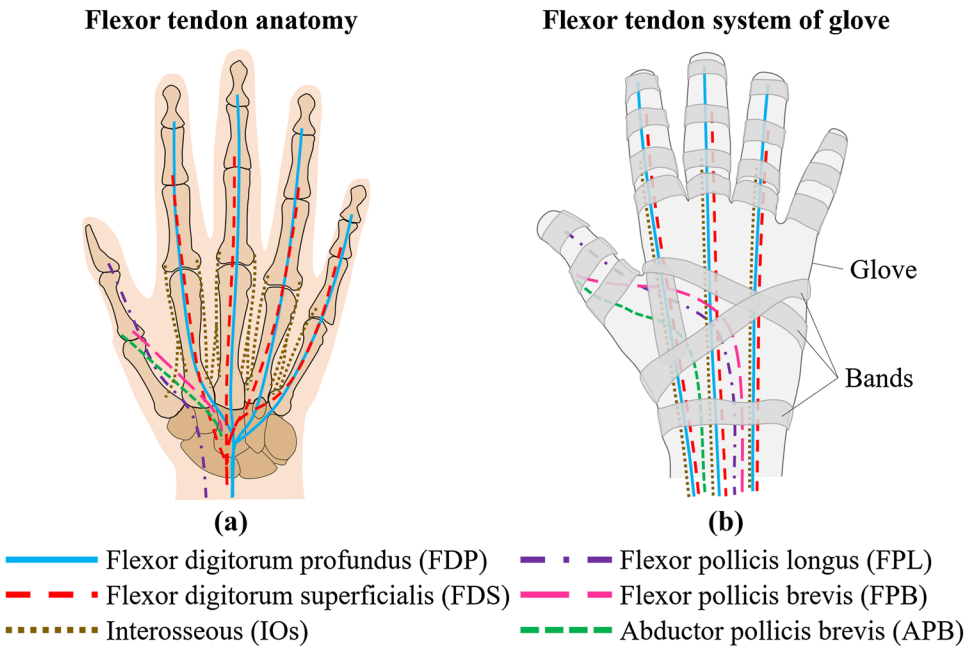

Fig. 3 Comparative illustration: **a** flexor anatomy of a human left hand from palmar view [25]; **b** tendon strucutre of the muscle glove for the left hand at palmar side

the sleeve. FDP, FDS and IOs insert to distal, middle and proximal phalanges separately and have direct control of DIP, PIP and MCP flexion respectively. In this design the salient features mentioned above were copied in order to realize the independent flexion of the three finger joints and to preserve the different functionalities of the three flexors. FDP is responsible for both precision handling and power grip, while FDS remains irrelevant for precision handling but plays an important role in power grip [23, 24]. IOs assist the two extrinsic flexors by controlling both DOF of the MCP joint: flexion/extension and abduction/adduction. As this paper mainly focus on their assistance by flexion, the IOs are simplified as simple flexors in the muscle glove. Extensor digitorum (ED) is the main extensor of the fingers. Its tendons insert into distal and middle phalanges on the dorsal side (see Fig. 4). Two strings were used to mimic the special structure of the ED-tendon, bounding them to the corresponding position of the glove (see Fig. 4b). Both extensor strings split into two slips over the phalanges to avoid large pressure on the finger, but still remain above the rotation axis of DIP, PIP and MCP joint to ensure extension effect.

The proposed design concept contains four strings (see Figs. 3b, 4b) to control the thumb motions. The four strings are mainly inspired by the following muscles: flexor pollicis longus (FPL), flexor pollicis brevis (FPB), abductor pollicis brevis (APB) and extensor pollicis longus (EPL). FPL and EPL are extrinsic muscles, while FPB and APB are intrinsic thumb muscles. FPL and FPB are responsible for thumb flexion and opposition. In the muscle glove, the FPL-string is mainly responsible for thumb flexion and assists the FPB-string in opposition. The FPB-string pulls the thumb in front of the palm without the flexion of thumb IP joint. APB is mainly responsible for thumb abduction and supports additionally thumb opposition. EPL extends and abducts the thumb. By grasping an object, APB-string conducts firstly palmar abduction for pre-grasp posture. FPL- and FPB-string then support the hand to seize the object firmly. Finally, EPL-string reposes the thumb and releases the object. Since the four strings can realize the key functions of the thumb by grasping, we do not replicate all the thumb muscles in the glove. Like IOs, FPB and APB are presented as extrinsic muscles in the muscle glove.

3.3 Pulleys

Pulleys are fibrous sheathes which fasten the tendon to the bone and ensure efficient transmission of muscle force. The muscle glove contains inelastic textile bands to replicate this function. As shown in Fig. 5, the bands transfer the pull force (F_{flex} and F_{ex}) of the string to a push force (F'_{flex} and F'_{ex}) which is directly applied on the finger at the opposite side of the corresponding string. The bands are sewed firmly to the glove and provide channels and attachment points for the strings. In order to produce a large torque with a small force, the moment arm is maximized by placing the bands, to which the strings are attached, at the head of the phalanges. The rest of the bands are mainly for holding the strings close to the fingers. The crossed bands in the palm aims for unconstrained contraction of intrinsic hand muscles by grasping (see Fig. 3).

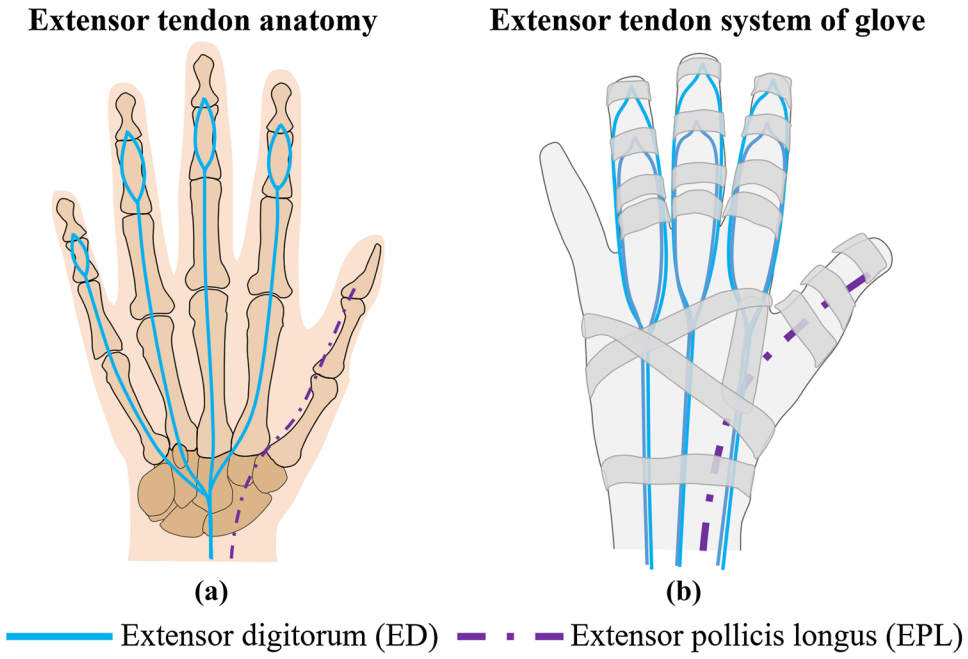

Fig. 4 Comparative illustration: **a** flexor anatomy of a human left hand from dorsal view [25]; **b** tendon strucutre of the muscle glove for the left hand at dorsal side

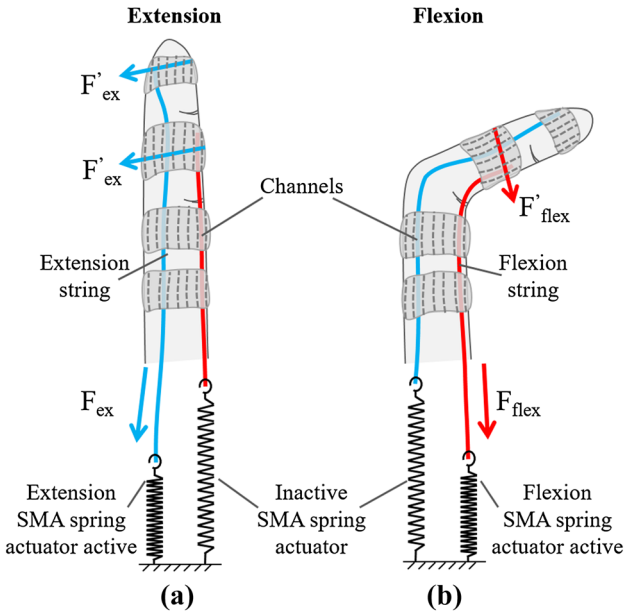

Fig. 5 Flexion and extension mechanism of the muscle glove (radial view): **a** by finger flexion, the flexor SMA spring actuator is activated and pulls the flexor string, while the extensor actuator is deactivated simultaneously; **b** it is reserved by finger extension

4 Artificial muscle

In this section, the design of the SMA spring actuator for our application is first explained, then the control of the SMA spring actuator is explained in respect of energy consumption.

4.1 Design of SMA spring actuator

The SMA spring actuators of the muscle glove are wound using Nitinol (NiTi) wire (Memory), whose hystersis is lower than the other SMA [26]. The SMA spring actuators are programmed to contract when electrically heated to their austenite temperature (the working temperature) and to remain inactive in room temperature. In regards to the wearable application, the austenite temperature of the SMA should not be significantly higher than the body temperature, as this would bring excess heat to the wearer. In addition, the inactive SMA spring should be as easily stretched as possible, so that the wearer can move freely when the glove is off. Consequently, a NiTi wire with an austenite temperature at about 60 °C was selected. The flexible sleeve, to which the SMA spring actuators are attached, is then made from thermal insulation textile to protect the user from excess heat.

For the muscle glove we are interested in a low-mass and small-size SMA spring actuator with a large spring rate. The spring rate k is determined by the following parameters: shear modulus G, wire diameter d, spring mean diameter D and the number of active coils n. Their relationship can be described by the following equation:

$$k = \frac{Gd^4}{8D^3n} \ . \tag{1}$$

The shear modulus G depends on the material properties. Wire diameter d, spring mean diameter D and the number of active coil n are decided according to the Eq. (1), aiming to maximize the spring rate k.

Thick wire can produce a large actuator force at a cost of being larger and heavier. Additionally, the string strength of the inactive SMA spring actuator also increase with a larger wire diameter. There are three diameters available for the selected NiTi wire: 0.21, 0.32 and 0.5 mm. Based on the considerations above, the 0.32 mm wire was selected to balance the tradeoffs.

In the case of the determined wire diameter, small mean spring diameter and reduced active spring coils call for large active spring strength but short stroke. In order to realize the desired finger motions, sufficient stroke length is necessary. By making tightly wound coils the required number of active coils can be minimized for a fixed stroke length. Under the prerequisite of meeting the requirement of stroke length for repeatable application, the minimum number of active coils for a minimum spring diameter was selected to produce as much actuator force as possible. Consequently, tightly wound SMA springs were made with a 1.8 mm outer diameter and 40 mm free length.

4.2 Control of SMA spring actuator

The low energy efficiency of SMA spring actuators prevent them from a wide range of applications. Pulse width modulation (PWM) signal is repoerted to be a solution to reducing energy consumption of SMA spring actuator [27]. A microcontroller (Infineon XMC 4500) is used to control the SMA spring actuator. It generates PWM signals to operate Logic level power MOSFETs (International Rectifier, IRLU2905ZPbF) to modulate the voltage which is applied to heat the SMA spring actuator. The controller regulates the power application by changing the duty cycle of the PWM signal. There are three control modes for the SMA spring actuators in the muscle glove: “on”, “hold” and “off”. The three modes are manually switched by pressing the corresponding buttons. The “on” mode is for activation and requires high power to heat the SMA spring as quickly as possible. As long as the working point is achieved, excess power will only produce unnecessary heat. To this end, the power application will be reduced in “hold” mode, aiming to remain on the working point with minimum power application. In “off” mode, the SMA actuator would be deactivated by cutting off its power supply.

Two tests were conducted to find out the suitable duty cycles of the PWM signal for the "on" and "hold" mode, leading to quick response and high energy efficiency. As shown in Fig. 6, the experimental set-up uses a rubber stretch sensor to observe the length change of the SMA spring actuator. At the beginning of the tests, the rubber sensor was held straight and unloaded while the SMA spring actuator was inactive with a stretched length of 5.8 cm. Then, the SMA spring, actuated by modulated voltage (5 V), contracted and pulled the rubber sensor to the maximum length. The electrical resistance of the rubber sensor increased as it is stretched. The initial length of the rubber sensor is 10.16 cm and its operation range is 40–50% elongation.

In the first test, the behavior of the SMA spring actuator was observed under stimulation of PWM signals with different duty cycles. The data recording started simultaneously with the PWM signal and ended after 15 s. As shown in Fig. 7, the stretch of the rubber sensor as well as the SMA spring contraction has three phases: acceleration, constant speed and deceleration. The constant speed and the acceleration of the SMA spring contractions strongly depend on the heating power determined by the duty cycle of the PWM signal. By 90% duty cycle the SMA spring actuator reacted significantly faster than by the other duty cycles. Under the stimulation of PWM signal with 90% duty cycle, the SMA spring entered the constant speed phase after 0.3 s and reached the maximum contraction in 2 s. This is suitable for laboratory tests to be conducted in the Sect. 5. Thus, the 90% duty cycle was selected for the "on" mode. For practical assembly tasks a higher voltage would be applied for a faster response time.

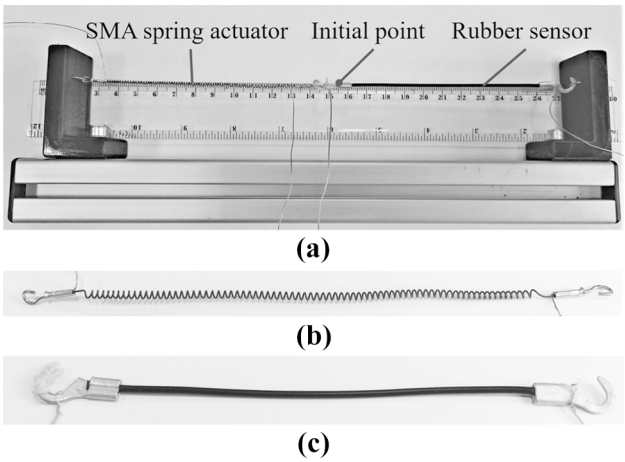

Fig. 6 **a** The experimental set-up: both the SMA actuator and the rubber sensor were fixed on one end, and connected to each other on the other end. The ruler was used to mark the initial point of zero displacement, ensuring the tests always start at the same point; **b** the SMA actuator; **c** the rubber sensor

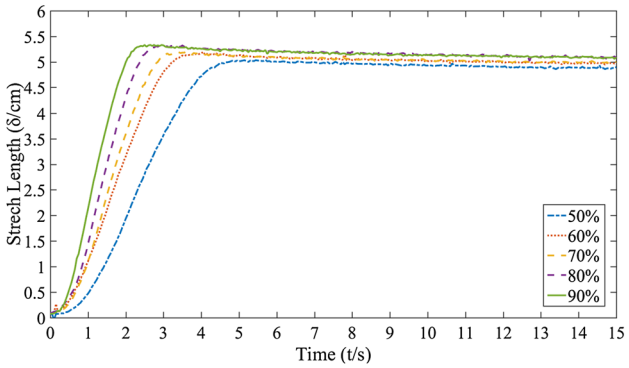

Fig. 7 The changing of the stretch length of the rubber sensor caused by the SMA spring actuator, stimulated by PWM signals with different duty cycles: from 50 to 90%

The second test aimed to find out the proper duty cycle for "hold" mode. According to the results from the first test, a PWM signal with 90% duty cycle was applied at the beginning for a quick actuation. The duty cycle was simultaneously turned down to different values (from 0 to 30%) when the maximum stretch length was achieved. Each test iteration took 50 s. The behavior of the SMA spring actuator is shown in Fig. 8. A balance between heating and cooling can already be seen by the 20% duty cycle inside the 50 s. Each test task in Sect. 5 for the muscle glove did not take longer than 50 s. Consequently, 20% is a reasonable setting for the hold mode in this work.

In addition, the curve of the 0% duty cycle shows that, the natural cooling process took place over time. That is to say, the SMA spring actuator is not completely inactive when powered off. Therefore, the muscle glove contains SMA spring actuators for both flexion and extension which provide counter force each other (see Fig. 5). A release, for instance, can be quickly realized after the grasp by simultaneously actuating the extension SMA spring and turning off the flexion SMA spring.

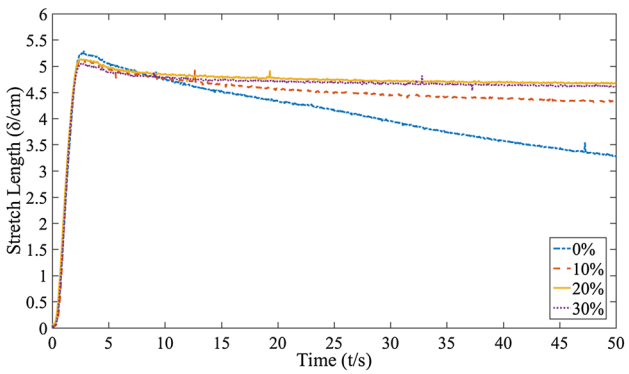

Fig. 8 The effects of PWM signals with different duty cycles (from 0 to 30%) by holding the maximum stretch length of the rubber sensor

5 Experimental evaluation

In order to evaluate our design concept we experimentally investigated the performance of the muscle glove, especially the functionality of the highly biomimetic soft structure, by free movement and grasping tasks. The glove was tested on the left hand of a healthy female subject. The subject sat in front of the table with forearm and hand resting on it. During all of the tasks with the active muscle glove the subject was instructed to relax the left hand completely. Voluntary finger movements of the subject was excluded by measuring EMG signals of the extrinsic hand muscles which are major contributors to finger movements [23]. The EMG measurement was made following the European Recommendations for Surface ElectroMyoGraphy [28].

5.1 Free movement performance

To assess the functionality of each string of the muscle glove and their collaboration, the following free movements were examined: four finger motions, four thumb motions and six gestures (see Figs. 9, 10, 11).

To evaluate the finger and thumb motions, the range of motion (ROM) of finger joints was measured by using computer-aided photographic goniometry. The measurement was done according to the procedure described in [29, 30]. Eight motions were regarded for the measurements. Both the ROM of the glove and the ROM of the subject were measured. Thus, each motion was performed in two different modes: (1) glove inactive, the subject performed the specified motion actively with the muscle force; (2) glove active, the muscle glove made the fingers move while the subject kept the left hand muscles relaxed. Each motion was conducted and photographed twice in each mode. The eight motions exerted by the muscle glove are exhibited in Figs. 9 and 10. The photographs were taken from a perpendicular viewpoint at the end of the motion. To ensure a comparable measurement result, the subject kept the inactive glove on when voluntarily performing the specified motions. When the muscle glove was set to inactive, it neither exerted active support force to the user, nor disturbed the voluntary motion of the user. The active ROMs of the muscle glove and the subject were calculated and comparatively presented in Table 2. In all the measured motions, except the flexion of finger PIP joint, the active ROM of the subject was achieved by the active muscle glove. The maximal flexion range of finger PIP joint achieved by the muscle glove was 81% of the active ROM of the subject. However, it covers the functional ROM according to the results of hand grip function test in Sect. 5.2 (Fig. 12). The optimization of the active ROM of finger PIP joint will be addressed in future work.

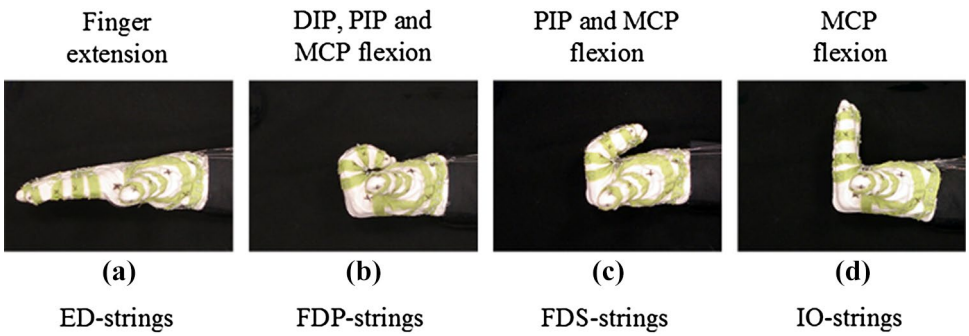

Fig. 9 Photographs of end postures of four finger motions exerted by the muscle glove: **a** hyperextension, **b** DIP, PIP and MCP flexion, **c** PIP and MCP flexion with DIP extension, **d** MCP flexion only. Each finger motion was exerted by only one type of strings: **a** ED-strings, **b** FDP-strings, **c** FDS-strings, **d** IO-strings. The thumb was pulled by the EPL-string to its maximal radial abduction position

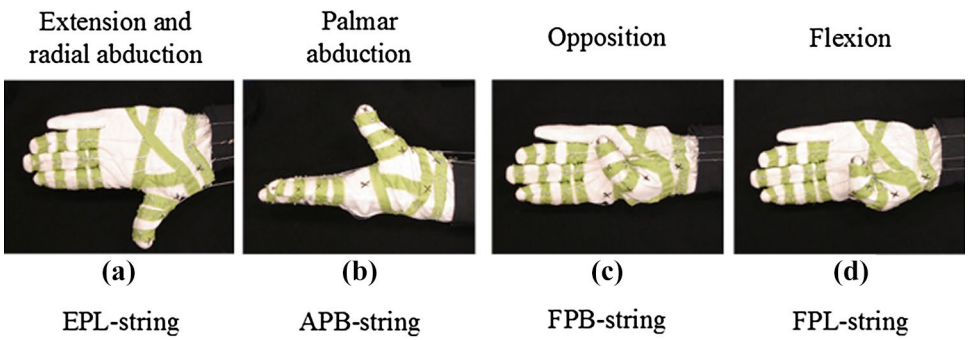

Fig. 10 Photographs of end postures of four thumb motions exerted by the muscle glove: **a** extension and radial abduction, **b** palmar abduction, **c** opposition, **d** flexion. Each thumb motion was exerted by only one string: **a** EPL-string, **b** APB-string, **c** FPB-string, **d** FPL-string. The fingers were extended by the ED-strings

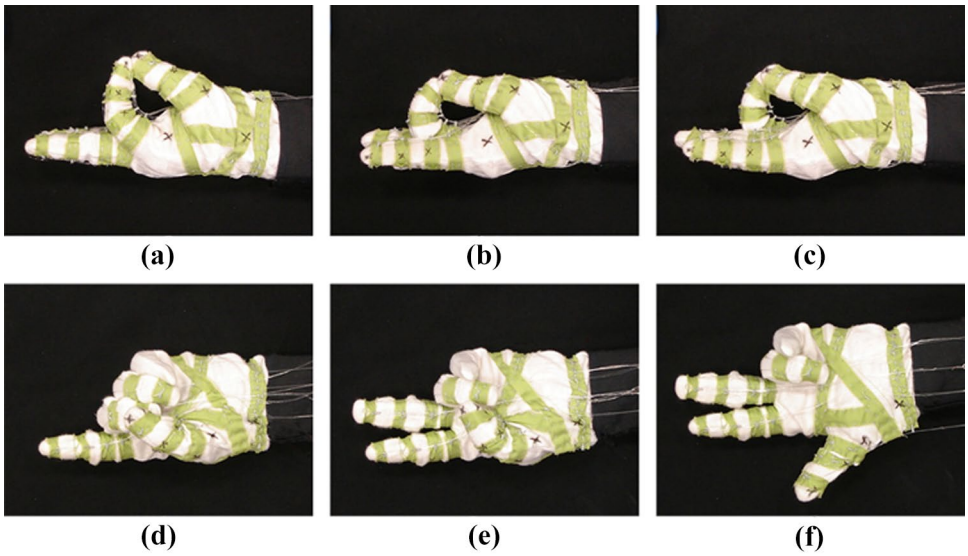

Fig. 11 Photographs of six gestures achieved by the muscle glove: **a**–**c** touching the tip of index, middle and ring finger respectively with the thumb tip, **d** only index finger extension, **e** index and middle finger extension, **f** only ring finger flexion

Table 2 Mean finger joint motion: active ROM of glove and subject

Joint motion	Glove	Subject
Index DIP extension/flexion	0°/59°	−7°/61°
Index PIP extension/flexion	−7°/72°	−9°/88°
Index MCP extension/flexion	−13°/86°	−13°/88°
Thumb CMC radial abduction	51°	52°
Thumb CMC palmar abduction	50°	51°
Thumb IP extension/flexion	−11°/64°	−14°/65°
Thumb MCP extension/flexion	0°/62°	0°/62°

The glove could be optimized by preserving more anatomical features of hand ligaments in two aspects: one is the form of the flexion pulleys, the other is the extension hood which is a special sheath for extensor tendons and also plays an important role in finger flexion.

The thumb opposition function and the collaboration of the digits were evaluated by performing six gestures in Fig. 11. Every gesture began from the relaxed hand position, and the muscle glove flexed or extended the digits to the predefined positions. As shown in Fig. 11a–e, the muscle glove can exert sufficient thumb opposition so that the thumb tip touches the tip and the middle phalange of the index, middle and ring finger. This confirms that the glove can achieve functional thumb opposition regarding the criterion of a clinical hand function test [31]. Thanks to the uncoupled control of the index, middle and ring finger, the muscle glove can bend and stretch the fingers either together (see Fig. 9) or separately (see Fig. 11). On this basis, work will be done in the future to realize advanced hand motions, e.g. in-hand manipulation. The unactuated little finger is observed to move passively with the other fingers due to finger independence [32]. This independence would be considered in later work when an active little finger is involved in the muscle glove.

5.2 Grasping performance

To evaluate the hand grip function achieved by the muscle glove, 14 grip tasks (Fig. 12) were conducted according to the grasp taxonomy in [33]. During the test, the subject relaxed the hand while the glove helped the subject to grip and hold 10 objects with different grasp postures. The ten objects weighed from 7.2 to 380.6 g. The 14 grasp types were achieved by the muscle glove with different string configurations. All the power grasp types ([a–f] and [k–m] in Fig. 12) were achieved by actuating FDP- and FDS-strings, while the types of precision grasps with thumb abduction ([g–j] in Fig. 12) were achieved by active FDP-strings only. This is consistent with the statement “FDP muscle is predominant by precision handling” in [23]. The grasp type (n) was achieved by IO- and FDS-strings. The 14 grip tasks suggest that the functional ROM of the hand is encompassed by the ROM of the muscle glove.

To quantitatively assess the supporting effect of the muscle glove, surface EMG sensors (Myon, Switzerland) were used to measure the activity of two flexion muscles in the forearm. The measurement was conducted during an 11 N hook grip which was performed in two modes: by the subjects muscle (glove inactive) and by the muscle glove (glove active). The hook grip force was measured by a KERN hanging scale CH (see Fig. 13b). Nine SMA spring actuators for three fingers (index, middle and ring finger) are involved in this test. Each finger was driven by three SMA spring actuators which are separately connected to the FDP-, FDS- and IO-string of the finger. 11 N was the maximum hook force produced by the nine SMA

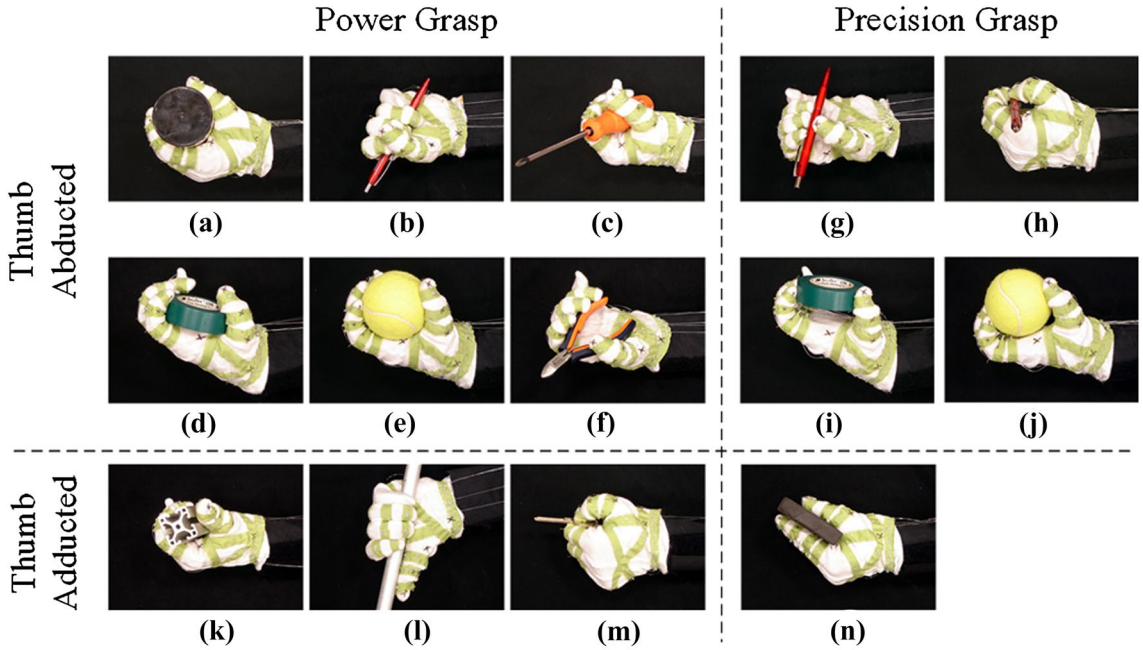

Fig. 12 Realized grasp types defined in taxonomy in [27]: **a** large diameter, **b** small diameter, **c** medium wrap, **d** power disk, **e** power sphere, **f** distal, **g** prismatic 3 finger, **h** writing tripod, **i** precision disk, **j** precision sphere, **k** adducted thumb, **l** fixed hook, **m** lateral and **n** parallel extension

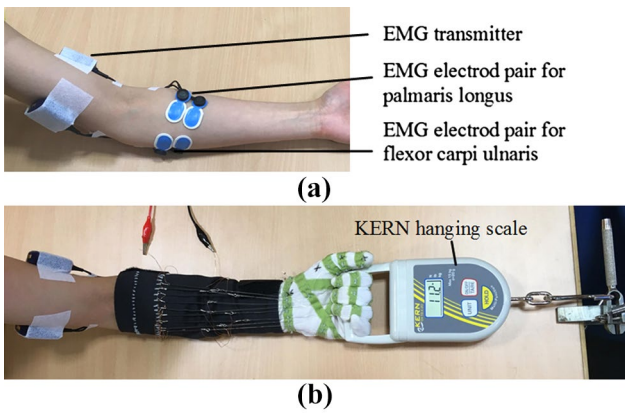

Fig. 13 Photograph of the experimental set-up: **a** the locations of two pairs of surface EMG electrodes; **b** the scale has a handle loop (15.03 mm deep and 9.46 mm thick) to be hand-held on one side and a steel hook on the other side. The scale was aligned with the subjects arm and fixed on the hook

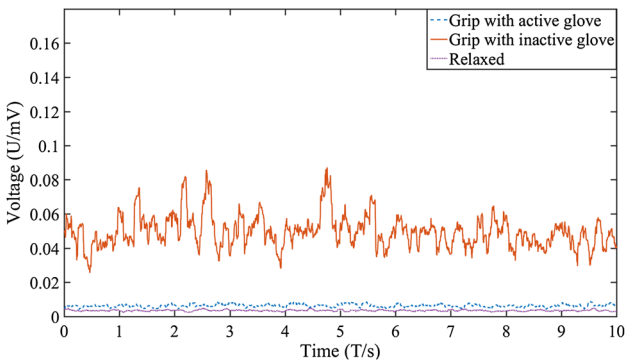

Fig. 14 EMG signal of left palmaris longus in three cases (top–down): 11 N hook grip with inactive glove, 11 N with active glove and relaxed

spring actuators. Larger forces can be created by adding more actuators per tendon string if necessary. The EMG signal was recorded at a frequency of 2000 Hz. The FDP and FDS muscle locate deeply under the skin and their activities cannot be detected directly using surface EMG, but can be detected as crosstalk over neighboring muscles. To get a reference measure, electrodes were placed over palmaris longus and flexor carpi ulnaris muscles for this test (see Fig. 13a). Recordings were taken in three cases: relaxed, grasping with muscle force (inactive muscle glove) and grasping with active muscle glove (see Figs. 14, 15). Three recordings were made for each condition. Each recording took 10 s and was followed by a 2 min rest. In the two cases of grasping, the recordings started simultaneously when the grip force reached about 11 N. Mean values are calculated and presented in Table 3. In the case of inactive glove the two muscles showed higher activity than in the case of active glove. This suggests that the muscle glove can augment the grip force for reduction in muscle stress.

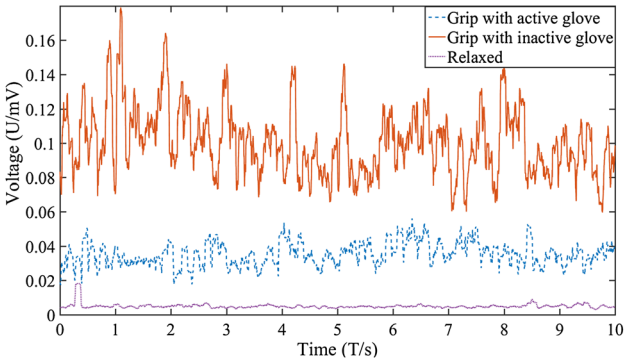

Fig. 15 EMG signal of left flexor carpi ulnaris in three cases (top–down): 11 N hook grip with inactive glove, 11 N with active glove and relaxed

Table 3 Mean values of the EMG signals of palmaris longus and flexor carpi ulnaris muscles in three cases: relaxed, grip with inactive glove and grip with active glove

	Relaxed (mV)	Grip with inactive glove (mV)	Grip with active glove (mV)
Left palmaris longus	0.0036	0.0497	0.0063
Left flexor carpi ulnaris	0.0046	0.1003	0.0353

5.3 Impact of FDS- and IO-strings on grasp

FDS and IO muscles uncouple the flexion of PIP and MCP joint from the flexion of DIP joint, which allows fine adjustment of each joint angle. This affects the efficiency of grasping in two aspects: grasp posture and grip force. Comparative experiments were conducted to investigate the effect. Firstly, the grasp posture performed by two different types of string configurations was compared: the first type of configuration contains only FDP-strings (see [a and b] in Fig. 16), while the second type involves FDS- and IO-strings (see [c and d] in Fig. 16). The glove is preset to the above mentioned configurations and aided the subject in grasping and holding the objects. Meanwhile, the subject was instructed to relax the affected (left) hand. As shown in Fig. 16, the grasp postures in (c) and (d) fit much better to the objects form than those in (a) and (b) by varying the PIP and MCP joint angles. The better matching between the grasp posture and the objects form allows secure grasp with more contact surface, thereby better friction for grasping. As a result, a secure grasp requires less force. To prove this, the maximal load mass of the two grasp postures based on the string configurations in (b) and (d) in Fig. 16 was measured. Each finger was driven by two SMA spring actuators in both cases. The handle size was 51.32 mm and the coefficient of friction between the glove and the object was under 0.3. The results

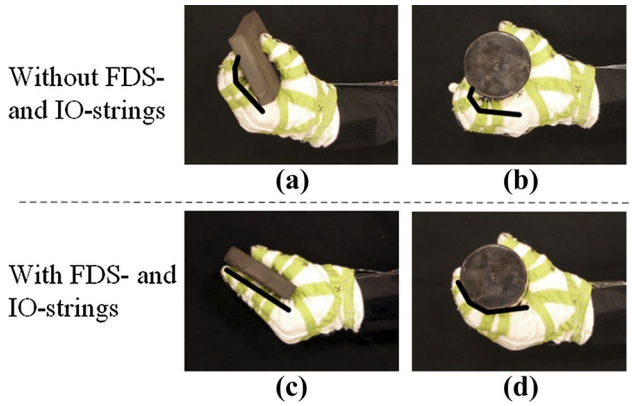

Fig. 16 Comparison of grasp postures under different string configurations: **a**, **b** only FDP-strings are actuated, two SMA actuator per tendon string; **c** FDS- and IO-strings are actuated, one actuator per tendon string; **d** FDP-and FDS-strings are actuated, one actuator per tendon string

Table 4 Maximal load mass by grasping with string configuration (b) and (d) from Fig. 16

String configuration	(b) FDP-strings only	(d) FDP- and FDS-string
Max. load mass	711 g	806 g

are shown in Table 4, with the same amount of tension produced by the SMA spring actuators the grasp posture (d) can hold heavier load mass, corresponding to more grip force. The efficiency of the force transmission, i.e. the ratio of grip force to muscle tension, is thus higher. This again suggests that involving FDS- and IO-strings to the muscle glove is important for the grasping efficiency. Moreover, the required tension for a grasp is better distributed to the finger phalanges through the FDS- and IO-strings. This reduces the pressure on the fingertip in comparison to the string configuration which contains only FDP-strings, especially when high tension is required.

6 Conclusion and future work

In this work, a muscle glove was designed and prototyped to preserve the salient functions of the human hand. The general approach of our proposed work was to identify the vital anatomical features of the human hand and to replicate these features in the muscle glove. This approach can also be applied to develop soft WR devices for other anatomical regions. The muscle glove provide the ability to augment grip force and reduce muscle stress. The proposed biomimetic design allows the muscle glove to achieve functional ROM of the human hand and to approach human-level dexterity. We extended the conventional tendon-pulley structure

from previous work by involving all of the critical tendons for finger flexion. This gains the following advantages:

- Uncoupling the flexion motions at the PIP, MCP and DIP joints allow more comprehensive hand movements
- Minimizing the mismatch between the grasp posture and the objects form, so that a more efficient force transmission from actuator to grip force
- The required tension is distributed to all finger phalanges, so that excessive pressure on one phalange, especially on the fingertip, would be averted when high tension are required.
- The capability of the muscle glove to flex the PIP and MCP joint without DIP joint flexion opens a new application area for it. Besides grasping support, the muscle glove can also be used by people who are not able to do advanced hand movements, e.g. in-hand manipulation.

In future work, we are planning to integrate sensors into the glove for an intuitive control of the motions and the force. Meanwhile, further study is needed to optimize the ROM of the PIP joint. To achieve advanced hand motion, like in-hand manipulation, further investigation is necessary into motion control of the human hand. In addition, the optimization of the SMA actuator and further biomechanical analysis will be conducted regarding practical needs in assembly tasks. Active supports for wrist and the little finger could also be considered.

Acknowledgements This research was conducted in the project "Smart ASSIST Smart, Adjustable, Soft and Intelligent Support Technologie" (16SV7114) and funded by the Federal Ministry of Education and Research (BMBF) program for an interdisciplinary build-up of competence in human machine interaction for demographic changes. Supervision is provided by VDI/VDE INNOVATION GmbH. The sole responsibility for the manuscript contents lies with the authors.

References

1. European Foundation for the Improvement of Living and Working Conditions and others (2014) Changes over time--first findings from the fifth European working conditions survey. Publications Office of the European Union
2. Barr AE, Barbe MF, Clark BD (2004) Work-related musculoskeletal disorders of the hand and wrist: epidemiology, pathophysiology, and sensorimotor changes. J Orthop Sports Phys Ther 34(10):610–627. doi:10.2519/jospt.2004.34.10.610
3. Bureau of labor statics: nonfatal occupational injuries and illnesses requiring days away from work, 2015 (2016). https://www.bls.gov/news.release/osh2.nr0.htm. Accessed 6 Dec 2016
4. Ikeuchi Y, Ashihara J, Hiki Y, Kudoh H, Noda T (2009) Walking assist device with bodyweight support system. In: 2009 IEEE/RSJ international conference on intelligent robots and systems, pp 4073–4079. doi:10.1109/IROS.2009.5354543
5. Otten B, Stelzer P, Weidner R, Argubi-Wollesen A, Wulfsberg JP (2016) A novel concept for wearable, modular and soft support systems used in industrial environments. In: 2016 49th Hawaii international conference on system sciences (HICSS), pp 542–550. doi:10.1109/HICSS.2016.74
6. Diftler M, Ihrke CA, Bridgwater LB, Davis DR, Linn DM, Laske EA, Ensley KG, Lee JH (2014) RoboGlove—a robonaut derived multipurpose assistive device. In: International conference on robotics and automation. Hong Kong, China
7. ExoHand—Festo corporate. https://www.festo.com/group/en/cms/10233.htm. Accessed 23 Nov 2016
8. Weidner R, Kong N, Wulfsberg JP (2013) Human hybrid robot: a new concept for supporting manual assembly tasks. Prod Eng 7(6):675–684. doi:10.1007/s11740-013-0487-x
9. Worsnopp T, Peshkin M, Colgate J, Kamper D (2007) An actuated finger exoskeleton for hand rehabilitation following stroke. In: 2007 IEEE 10th international conference on rehabilitation robotics, pp 896–901. doi:10.1109/ICORR.2007.4428530
10. Chiri A, Vitiello N, Giovacchini F, Roccella S, Vecchi F, Carrozza MC (2012) Mechatronic design and characterization of the index finger module of a hand exoskeleton for post-stroke rehabilitation. IEEE/ASME Trans Mechatron 17(5):884–894. doi:10.1109/TMECH.2011.2144614
11. Brown P, Jones D, Singh S, Rosen J (1993) The exoskeleton glove for control of paralyzed hands. In: [1993] Proceedings IEEE international conference on robotics and automation, pp 642–647. IEEE Comput Soc Press. doi:10.1109/robot.1993.292051
12. Wege A, Hommel G (2005) Development and control of a hand exoskeleton for rehabilitation of hand injuries. In: 2005 IEEE/RSJ international conference on intelligent robots and systems, pp 3046–3051. doi:10.1109/IROS.2005.1545506
13. Ueki S, Kawasaki H, Ito S, Nishimoto Y, Abe M, Aoki T, Ishigure Y, Ojika T, Mouri T (2012) Development of a hand-assist robot with multi-degrees-of-freedom for rehabilitation therapy. IEEE/ASME Trans Mechatron 17(1):136–146. doi:10.1109/TMECH.2010.2090353
14. Fontana M, Dettori A, Salsedo F, Bergamasco M (2009) Mechanical design of a novel hand exoskeleton for accurate force displaying. In: Robotics and automation, 2009. ICRA '09. IEEE international conference On, pp 1704–1709. doi:10.1109/ROBOT.2009.5152591
15. Delph MA, Fischer SA, Gauthier PW, Luna CHM, Clancy EA, Fischer GS (2013) A soft robotic exomusculature glove with integrated sEMG sensing for hand rehabilitation. In: Rehabilitation robotics (ICORR), 2013 IEEE international conference On, pp 1–7. doi:10.1109/ICORR.2013.6650426
16. In H, Kang BB, Sin M, Cho KJ (2015) Exo-Glove: a wearable robot for the hand with a soft tendon routing system. IEEE Robotics Autom Mag 22(1):97–105. doi:10.1109/MRA.2014.2362863
17. Nilsson M, Ingvast J, Wikander J, von Holst H (2012) The soft extra muscle system for improving the grasping capability in neurological rehabilitation. In: 2012 IEEE-EMBS conference on biomedical engineering and sciences, pp 412–417. doi:10.1109/IECBES.2012.6498090
18. Polygerinos P, Wang Z, Galloway KC, Wood RJ, Walsh CJ (2015) Soft robotic glove for combined assistance and at-home rehabilitation. Rob Auton Syst 73:135–143. doi:10.1016/j.robot.2014.08.014
19. Sasaki D, Noritsugu T, Takaiwa M, Yamamoto H (2004) Wearable power assist device for hand grasping using pneumatic artificial rubber muscle. In: Robot and human interactive communication, 2004. ROMAN 2004. 13th IEEE international workshop On, pp 655–660. doi:10.1109/ROMAN.2004.1374840
20. Pons JL (ed) (2008) Wearable robots: biomechatronic exoskeletons. Wiley, Hoboken, NJ
21. Dittmer DK, Buchal RO, Dawn E. MacArthur (1993) The SMART wrist-hand orthosis (WHO) for quadriplegic patients. J Prosthet Orthot 5(3):73

22. Labeled parts of the hand. http://gemn.dvrlists.com/labeled-parts-of-the-hand/. Accessed 10 Sep 2016
23. Long C, Conrad PW, Hall EA, Furler SL (1970) Intrinsic–extrinsic muscle control of the hand in power grip and precision handling. J B Jt Surg 52(5):853–867
24. Brand P, Beach R, Thompson D (1981) Relative tension and potential excursion of muscles in the forearm and hand. J Hand Surg 6(3):209–219. doi:10.1016/S0363-5023(81)80072-X
25. Gilroy AM, MacPherson BR, Voll MM, Wesker K, Schünke M (eds) (2016) Atlas of anatomy, 3rd edn. Thieme, New York
26. Pruski A, Kihl H (1993) Shape memory alloy hysteresis. Sens Actuator A Phys 36(1):29–35. doi:10.1016/0924-4247(93)80137-6
27. Ma N, Song G (2003) Control of shape memory alloy actuator using pulse width modulation. Smart Mater Struct 12(5):712–719. doi:10.1088/0964-1726/12/5/007
28. Hermens HJ, Freriks B, Merletti R, Stegeman D, Stegeman D, Blok J, Rau G, Disselhorst-Klug C, Hägg G (1999) European recommendations for surface electromyography. Roessingh Res Dev 8(2):13–54
29. Crasto JA, Sayari AJ, Gray RRL, Askari M (2015) Comparative analysis of photograph-based clinical goniometry to standard techniques. Hand 10(2):248–253. doi:10.1007/s11552-014-9702-2
30. Georgeu G (2002) Lateral digital photography with computer-aided goniometry versus standard goniometry for recording finger joint angles. J Hand Surg 27(2):184–186. doi:10.1054/jhsb.2001.0692
31. Kapandji A (1986) Clinical test of apposition and counter-apposition of the thumb. Ann De Chir De La Main 5(1):67–73
32. Lang CE (2004) Human finger independence: limitations due to passive mechanical coupling versus active neuromuscular control. J Neurophysiol 92(5):2802–2810. doi:10.1152/jn.00480.2004
33. Feix T, Romero J, Schmiedmayer HB, Dollar AM, Kragic D (2016) The GRASP taxonomy of human grasp types. IEEE Trans Hum Mach Syst 46(1):66–77. doi:10.1109/THMS.2015.2470657